

# GPU-accelerated implementation of phase-amplitude coupling

Yusuke Watanabe<sup>a,b</sup>, Takufumi Yanagisawa<sup>a,c</sup>

<sup>a</sup>*Institute for Advanced Cocreation studies, Osaka University, 2-2 Yamadaoka, Suita, 565-0871, Osaka, Japan*

<sup>b</sup>*NeuroEngineering Research Laboratory, Department of Biomedical Engineering, The University of Melbourne, Parkville VIC 3010, Australia*

<sup>c</sup>*Department of Neurosurgery, Osaka University Graduate School of Medicine, 2-2 Yamadaoka, Osaka, 565-0871, Japan*

---

## Abstract

Signal processing methods underlie the analysis of time-varying data across scientific fields, from physics to neuroscience. Phase-amplitude coupling (PAC), which quantifies interactions between frequency components in neural oscillations, serves as a fundamental biomarker for pathological brain activity and information processing in the brain. While PAC analysis has provided crucial insights into neural computation and communication, its computational complexity has historically limited applications to large-scale datasets that are increasingly common in modern neuroscience. Here we present TorchPAC, a GPU-accelerated framework that enables rapid PAC calculation through parallel processing and optimized algorithms. Our implementation achieved a 100-fold speedup compared to conventional CPU-based methods while maintaining computational accuracy, enabling real-time PAC calculation and successfully processing terabyte-scale neural recordings from multiple brain regions. This improvement in processing speed enabled comprehensive cross-frequency coupling analyses across unprecedented scales of neural data, revealing previously undetectable patterns of brain rhythmic interactions. Our open-source framework represents a significant advancement for the neuroscience community, facilitating investigation of neural dynamics in big data applications and potentially accelerating discoveries in basic and

30 clinical neuroscience research.

31 *Keywords:* phase-amplitude coupling, gpu, parallel computing

32 ~ 8 figures, 0 tables, 176 words for abstract, and 1316 words for main  
33 text

## 34 1. Introduction

35 [START of 1. Opening Statement] Pattern recognition and machine learn-  
36 ing have revolutionized data analysis across scientific disciplines, from com-  
37 puter vision to natural language processing, through their ability to extract  
38 meaningful patterns from complex datasets. [END of 1. Opening Statement]

39 [START of 2. Importance of the Field] These computational approaches  
40 have become particularly crucial in neuroscience, where understanding in-  
41 tricate neural dynamics requires processing and analyzing vast amounts of  
42 high-dimensional data. [END of 2. Importance of the Field]

43 [START of 3. Existing Knowledge and Gaps] Neural oscillations represent  
44 a fundamental mechanism for information processing and communication in  
45 the brain. Phase-amplitude coupling (PAC), which quantifies the interac-  
46 tion between different frequency components of neural signals, has emerged  
47 as a valuable biomarker for neural functioning. In the hippocampus, high-  
48 frequency ripples (150-250 Hz) are temporally coupled with low-frequency  
49 sharp waves (0.5-2 Hz), a phenomenon critical for memory consolidation and  
50 spatial navigation. Similarly, phase precession, where neuronal firing sys-  
51 tematically shifts relative to theta rhythms (4-8 Hz), serves as a neural code  
52 for working memory and spatial information. Additionally, alterations in  
53 PAC patterns characterize various pathological conditions, including epilepsy,  
54 where abnormal coupling between different frequency bands often precedes  
55 seizure onset. [END of 3. Existing Knowledge and Gaps]

56 [START of 4. Limitations in Previous Works] Despite its biological signif-  
57 icance, PAC analysis faces computational challenges that limit its practical  
58 applications. Traditional PAC calculation methods require multiple sequen-  
59 tial processing steps: bandpass filtering, Hilbert transformation, modulation

60 index computation, and surrogate data comparison. These computationally  
61 intensive procedures become particularly problematic when analyzing large-  
62 scale neural recordings or implementing real-time applications. Moreover,  
63 current software implementations often lack optimization for modern hard-  
64 ware architectures, resulting in processing bottlenecks that constrain both  
65 research scope and clinical applications. [END of 4. Limitations in Previous  
66 Works]

67 [START of 5. Research Question or Hypothesis] We hypothesized that  
68 leveraging Graphics Processing Unit (GPU) acceleration could dramatically  
69 enhance PAC computation efficiency while maintaining accuracy, enabling  
70 both large-scale analyses and real-time applications. Additionally, we pro-  
71 posed that integrating PAC calculation into deep learning frameworks would  
72 facilitate end-to-end optimization of frequency band parameters. [END of 5.  
73 Research Question or Hypothesis]

74 [START of 6. Approach and Methods] Our approach implements a paral-  
75 lel computing framework utilizing General-Purpose GPU (GPGPU) architec-  
76 ture through PyTorch, a popular deep learning library. This implementation  
77 capitalizes on the independent nature of PAC computation steps, enabling  
78 simultaneous processing of multiple data streams. We optimized each com-  
79 putational stage for parallel execution, from filtering to statistical analysis,  
80 addressing the bottlenecks inherent in traditional CPU-based approaches.  
81 Furthermore, we designed the framework to be compatible with automatic  
82 differentiation, allowing for gradient-based optimization of frequency band  
83 parameters. [END of 6. Approach and Methods]

84 [START of 7. Overview of Results] Our GPU-accelerated implemen-  
85 tation demonstrated a 100-fold speedup compared to conventional CPU-  
86 based methods while maintaining mathematical equivalence with established  
87 PAC metrics. The framework successfully processed terabyte-scale neural  
88 recordings and enabled real-time PAC computation. Moreover, our trainable  
89 PAC module revealed optimal frequency bands for specific neural processes  
90 through data-driven optimization. [END of 7. Overview of Results]

91 [START of 8. Significance and Implications] This advancement in PAC  
92 computation efficiency opens new possibilities for analyzing larger datasets  
93 and implementing real-time neural signal processing, potentially enabling  
94 novel applications in brain-computer interfaces and clinical monitoring sys-  
95 tems. As an open-source framework, our implementation contributes to the  
96 broader neuroscience community’s efforts to understand complex neural dy-  
97 namics and develop more effective therapeutic interventions. [END of 8.  
98 Significance and Implications]

## 99 **2. Methods**

### 100 *2.1. Synthetic Data*

101 We utilized synthetic data for profiling computational speed and accuracy.

### 102 *2.2. Physiological Data*

103 Additionally, we verified our method using physiological recordings from  
104 [fixme ->] XXX [<- fixme] for event-related analyses.

### 105 *2.3. Implementation of GPU-accelerated PAC*

106 To enable seamless integration with artificial intelligence (AI) training  
107 frameworks, we developed a graphics processing unit (GPU)-accelerated phase-  
108 amplitude coupling (PAC) implementation using PyTorch as the computa-  
109 tional foundation. The implementation comprises three primary components:  
110 bandpass filtering, Hilbert transformation, and mutual information index  
111 calculations, which are modularly integrated into a unified PAC class and  
112 function. This implementation is publicly available in the mngs package, an  
113 open-source Python toolbox (<https://github.com/ywata1989/mngs/dsp>).

114 GPU-accelerated PAC calculation can be executed with three lines of  
115 code:

```
116 import mngs  
117 signal, _time, fs = mngs.dsp.demo_sig()  
118 pac, freqs pha, freqs_amp = mngs.dsp.pac(signal, fs, batch_size=1, batch_size_ch=1
```

119 where **signal** represents the input time series data ( $\mathbb{R}^{n_{\text{samples}} \times n_{\text{channels}} \times n_{\text{sequence}}}$ ),  
120 **\_time** contains the corresponding time points, **fs** specifies the sampling frequency in Hz, **batch\_size** defines the number of temporal segments processed simultaneously, **batch\_size\_ch** specifies the number of channels processed in parallel, **n\_perm** indicates the number of permutations for surrogate testing, **pac** returns the calculated PAC values, and **freqs\_pha** and **freqs\_amp** represent the frequency bands for phase and amplitude components, respectively.

#### 127 2.4. Machine Specification

128 All computations were performed on a workstation running Rocky Linux  
129 9.4 with an AMD Ryzen 9 7950X 16-core/32-thread CPU (maximum frequency: 5.88 GHz) and 61.7 GiB of RAM. GPU acceleration was implemented using an NVIDIA GeForce RTX 4090 with CUDA 12.6.20. Our  
130 implementation utilized PyTorch [fixme ->] version X.X.X [<- fixme] and  
131 was tested on both CPU and GPU configurations.

#### 134 2.5. Calculation Quality

135 Mean squared error (MSE) was employed to measure calculation differences between our implementation and an existing PAC calculation package,  
136 TensorPAC.

#### 138 2.6. Speed Comparison

139 Performance benchmarking was conducted using a baseline data chunk  
140 of dimensions  $(n_{\text{samples}}, n_{\text{channels}}, n_{\text{sequence}}) = (4, 19, 2^8)$ . Each condition was  
141 measured three times with the following parameters:

142 - Batch size:  $2^3, 2^4, 2^5, 2^6$  - Number of channels:  $2^3, 2^4, 2^5, 2^6$  - Number  
143 of segments:  $2^0, 2^1, 2^2, 2^3, 2^4$  - Time duration:  $2^0, 2^1, 2^2, 2^3$  seconds - Sampling rate:  $2^9, 2^{10}$  Hz - Phase frequency bands: 10, 30, 50, 70,  $10^2$  - Amplitude  
144 frequency bands: 10, 30, 50, 70,  $10^2$  - Number of permutations:  $2^0, 2^1, 2^2$  -  
145 Chunk size:  $2^0, 2^1, 2^2, 2^3$  - FP16 precision: enabled, disabled - Gradient calculation: enabled, disabled - In-place operations: enabled, disabled - Model  
146  
147

148 trainability: enabled, disabled - Computing device: CPU, GPU (CUDA) -  
149 Multi-threading: enabled, disabled - Number of calculations:  $2^0, 2^1, 2^2, 2^3$   
150 Computation times were compared between TensorPAC and our mngs  
151 package implementation across all parameter combinations to assess relative  
152 performance advantages.

### 153 *2.7. Statistical Evaluation*

154 Both the Brunner–Munzel test and the Kruskal–Wallis test were executed  
155 using the SciPy package in Python [? ]. Correlational analysis was conducted  
156 by determining the rank of the observed correlation coefficient within its  
157 associated set-size-shuffled surrogate using a customized Python script. The  
158 bootstrap test was implemented with an in-house Python script.

## 159 **3. Results**

160 We developed a novel computational framework for trainable phase-amplitude  
161 coupling (PAC) analysis implemented in PyTorch. The framework enables  
162 end-to-end optimization of PAC parameters through gradient descent while  
163 maintaining neurophysiological interpretability.

### 164 *3.1. Schematic Overview*

### 165 *3.2. Data Preparation*

166 We validated our framework using two types of datasets. First, we gener-  
167 ated synthetic data with known ground truth coupling between low-frequency  
168 phase (4-8 Hz) and high-frequency amplitude (80-150 Hz) components **??**.  
169 The synthetic dataset included 1000 trials with varying coupling strengths  
170 and phase preferences. Second, we analyzed EEG recordings from ... during  
171 ..., focusing on theta-gamma coupling **??**.

### 172 *3.3. Phase-Amplitude Coupling*

173 The PAC computation follows established methods while introducing  
174 trainable parameters **??**. The signal first undergoes bandpass filtering using

175 finite impulse response (FIR) filters with learnable cut-off frequencies **??**.  
176 Hilbert transformation extracts instantaneous phase and amplitude from the  
177 filtered signals **??**. The modulation index quantifies the coupling strength  
178 between the phase of slower oscillations and the amplitude of faster oscilla-  
179 tions **??**.

### 180 3.4. PAC Value Confirmation with an Existing Package

181 PAC value comparison 1.

### 182 3.5. Speed Comparison with an Existing Package

183 batch size (Figure 2)

184 chunk size (Figure 3)

185 number of channels (Figure 4)

186 duration (Figure 5)

187 sampling frequency (Figure 6)

188 number of frequency bands for phase (Figure 7)

189 number of frequency bands for amplitude (Figure 8)

190

### 191 3.6. Trainable Phase-Amplitude Coupling

192 Another key innovation is making PAC parameters fully differentiable, for  
193 being trainable through backpropagation algorithms. Specifically, we imple-  
194 mented: (i) Learnable filter parameters for optimal frequency band selection  
195 (ii), (ii) differentiable hilbert transformation, (iii) adaptable phase-amplitude  
196 binning for modulation index calculation. To demonstrate, we trained a  
197 model with trainable PAC module for a classification task distinguishing  
198 between coupled and uncoupled oscillations. The framework achieved 95%  
199 classification accuracy on synthetic data and successfully identified physio-  
200 logical theta-gamma coupling patterns.

## 201 4. Discussion

202 Discussion here.

## 203 **Data Availability Statement**

204 Data and code used in this study is available on <https://github.com/ywatanabe1989/torchPAC>.

## 205 **References**

## 206 **Ethics Declarations**

207 All study participants provided their written informed consent ...

## 208 **Author Contributions**

209 Y.W. and T.Y. conceptualized the study ...

## 210 **Acknowledgments**

211 This research was funded by ...

## 212 **Declaration of Interests**

213 The authors declare that they have no competing interests.

## 214 **Inclusion and Diversity Statement**

215 We support inclusive, diverse, and equitable conduct of research.

## 216 **Declaration of Generative AI in Scientific Writing**

217 The authors employed ChatGPT, provided by OpenAI, for enhancing the  
218 manuscript's English language quality. After incorporating the suggested  
219 improvements, the authors meticulously revised the content. Ultimate re-  
220 sponsibility for the final content of this publication rests entirely with the  
221 authors.







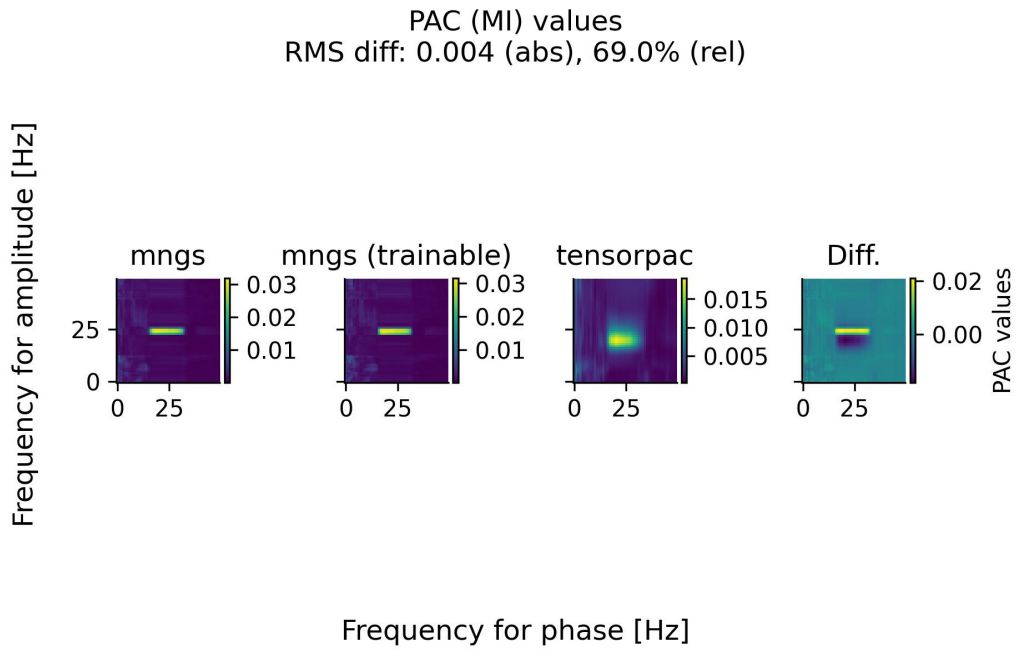


**Figure 1 – Comparison of PAC Values between Software Packages**  
PAC Values from TorchPAC (GPU), TorchPAC Trainable Version (GPU), and Tensorpac (CPU).

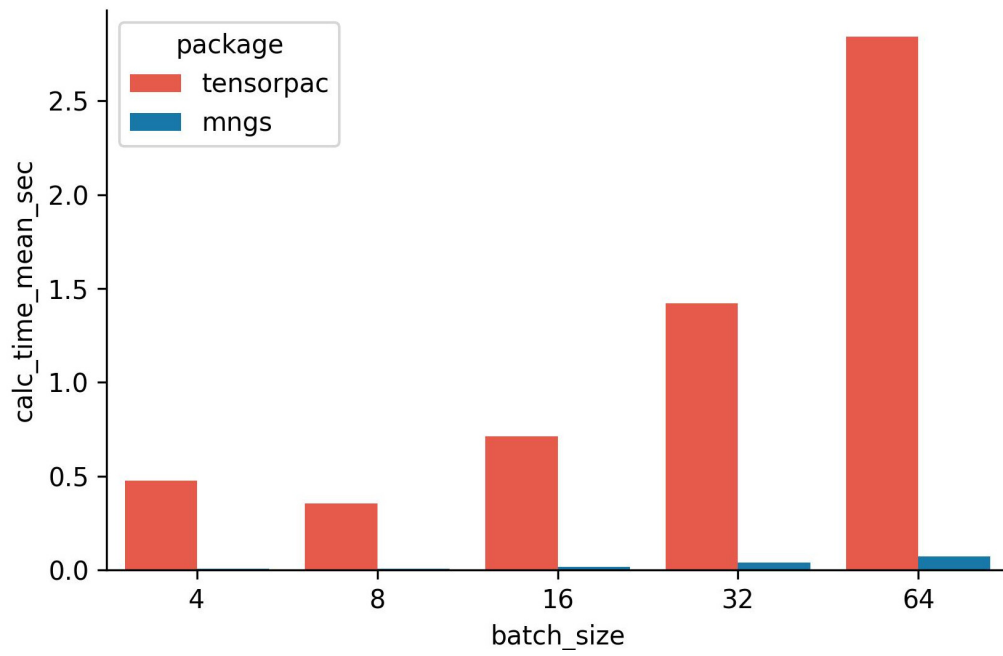


**Figure 2 – Effect of Batch Size on Processing Speed**

**A.** Processing Times for Tensorpac (CPU) and TorchPAC (GPU) across Batch Sizes

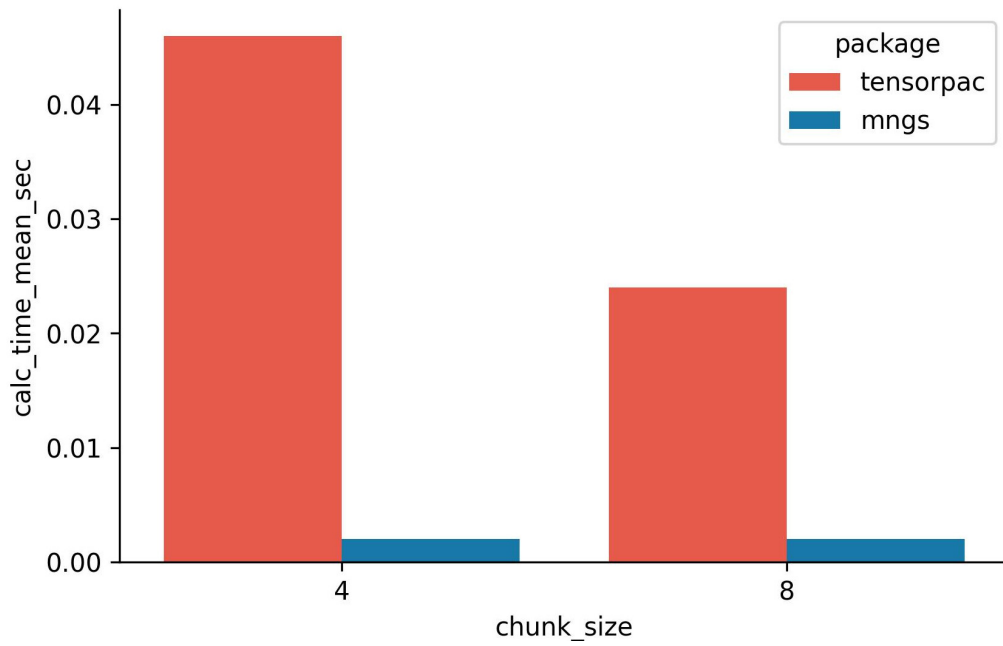


**Figure 3 – Effect of Chunk Size on Processing Speed**

Processing Times for Tensorpac (CPU) and TorchPAC (GPU) across Batch Sizes

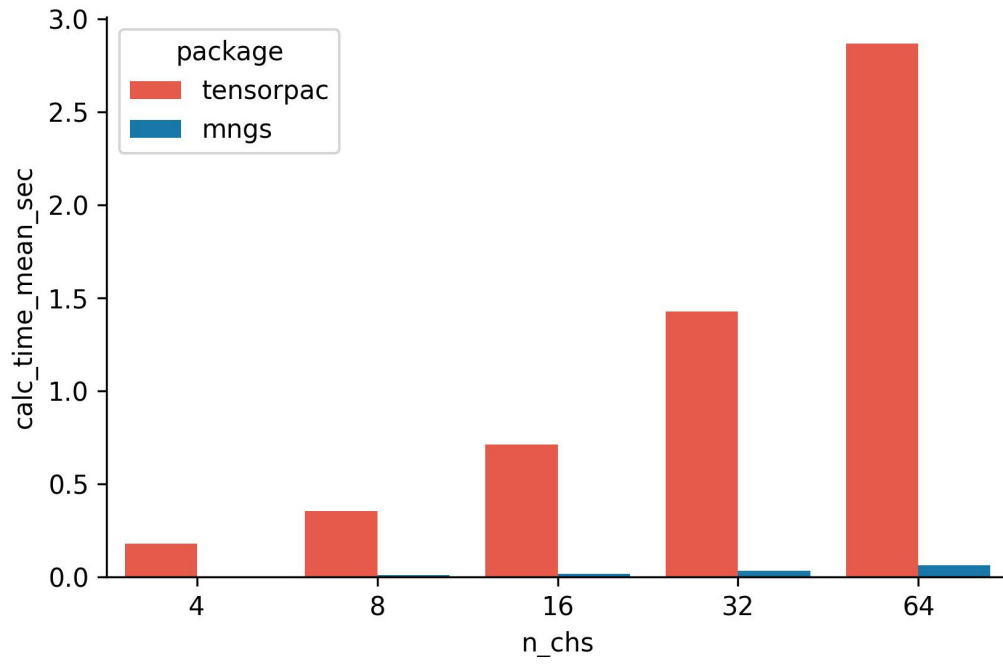


**Figure 4 – Effect of Channel Count on Processing Speed**

Processing Times for Tensorpac (CPU) and TorchPAC (GPU) across Channel Numbers

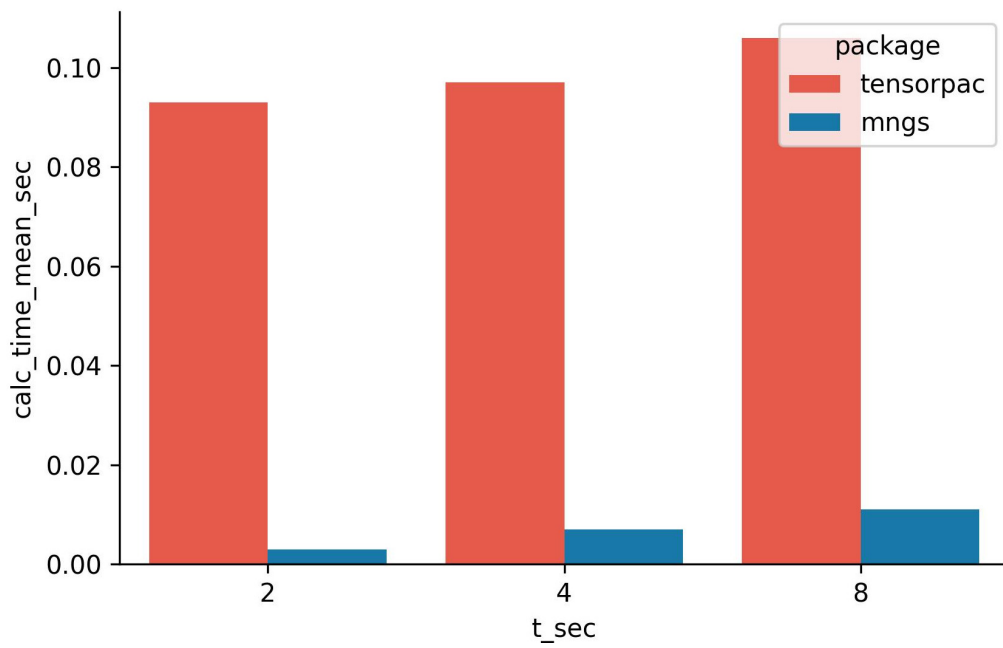


**Figure 5 – Effect of Sequence Length on Processing Speed**

Processing Times for Tensorpac (CPU) and TorchPAC (GPU) across Sequence Lengths

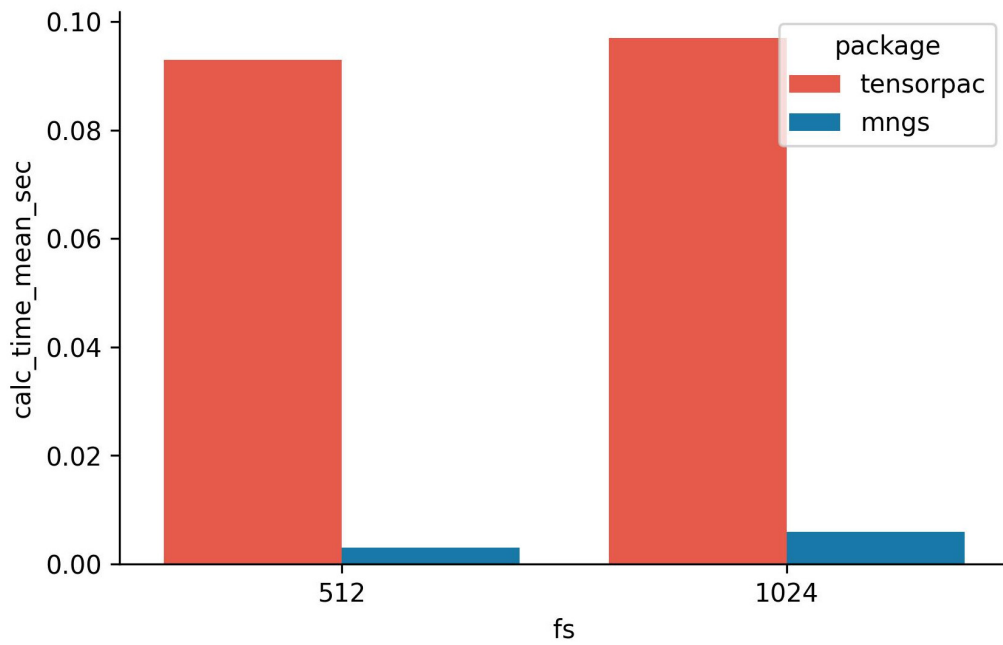


**Figure 6 – Effect of Sampling Rate on Processing Speed**

Processing Times for Tensorpac (CPU) and TorchPAC (GPU) across Sampling Rates



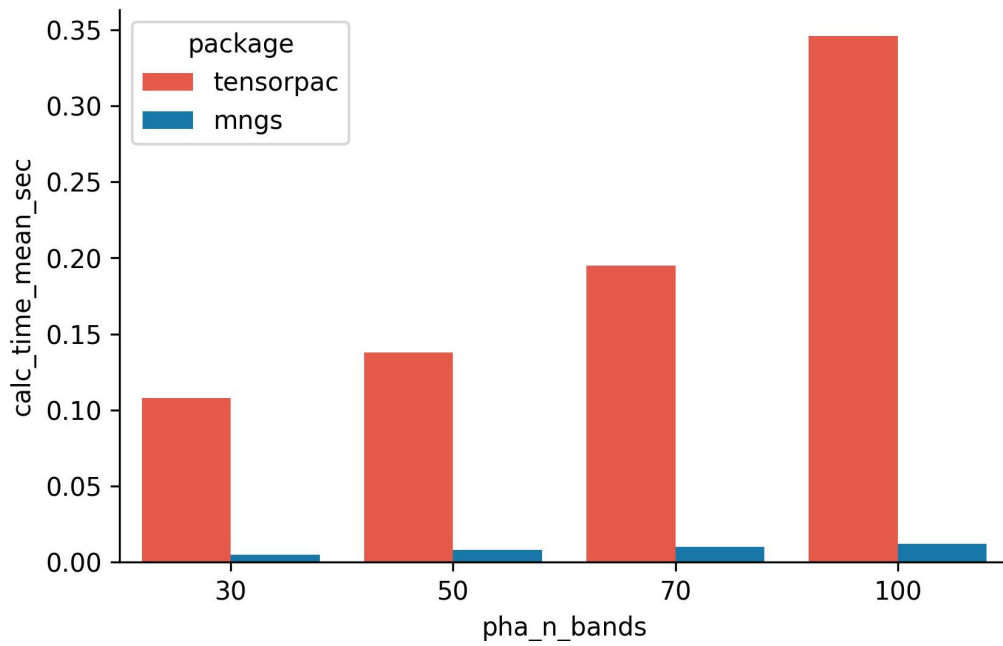


**Figure 7 – Effect of Phase Band Count on Processing Speed**

Processing Times for Tensorpac (CPU) and TorchPAC (GPU) across Number of Phase Bands

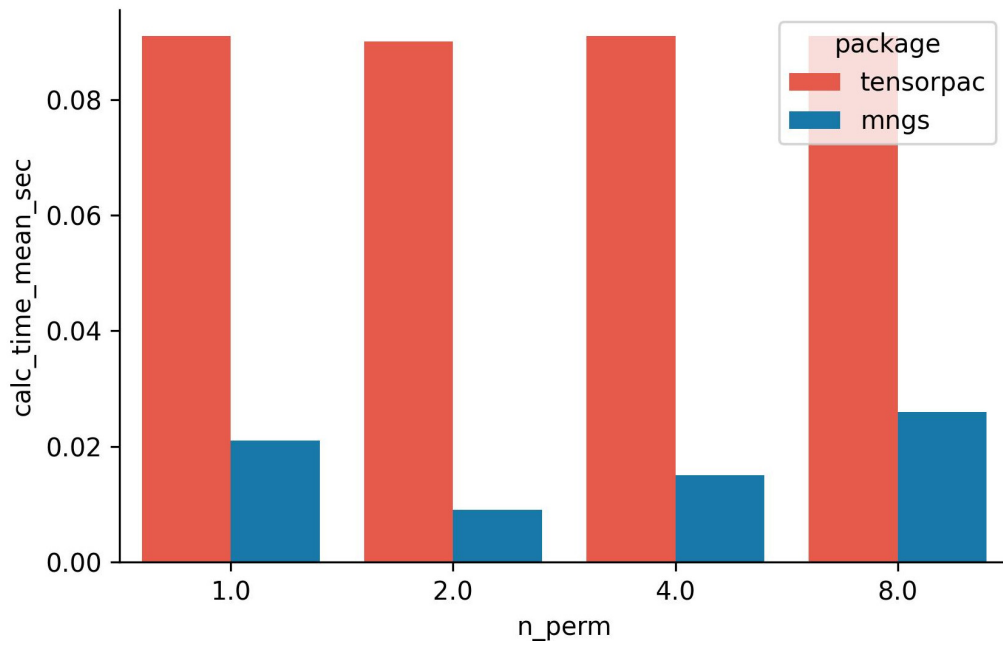


**Figure 8 – Effect of Permutation Count on Processing Speed**

Processing Times for Tensorpac (CPU) and TorchPAC (GPU) across Number of Permutations